



Three dimensional spatial separation of cells in response to microtopography



Alexandre Leclerc^a, Dominique Tremblay^a, Sebastian Hadjiantoniou^a,
Nickolay V. Bukoreshtliev^a, Jacob L. Rogowski^a, Michel Godin^{a,b}, Andrew E. Pelling^{a,c,d,*}

^a Department of Physics, MacDonald Hall, 150 Louis Pasteur, University of Ottawa, Ottawa, ON K1N 6N5, Canada

^b Ottawa-Carleton Institute for Biomedical Engineering, Colonel By Hall, 161 Louis Pasteur, University of Ottawa, Ottawa, ON K1N 6N5, Canada

^c Department of Biology, Gendron Hall, 30 Marie Curie, University of Ottawa, Ottawa, ON K1N 6N5, Canada

^d Institute for Science, Society and Policy, Simard Hall, 60 University, University of Ottawa, Ottawa, ON K1N 6N5, Canada

ARTICLE INFO

Article history:

Received 15 June 2013

Accepted 12 July 2013

Available online 27 July 2013

Keywords:

Microtopography
Confinement
Spatial separation
Co-culture

ABSTRACT

Cellular organization, migration and proliferation in three-dimensions play a critical role in numerous physiological and pathological processes. Nano- and micro-fabrication approaches have demonstrated that nano- and micro-scale topographies of the cellular microenvironment directly impact organization, migration and proliferation. In this study, we investigated these dynamics of two cell types (NIH3T3 fibroblast and MDCK epithelial cells) in response to microscale grooves whose dimensions exceed typical cell sizes. Our results demonstrate that fibroblasts display a clear preference for proliferating along groove ridges whereas epithelial cells preferentially proliferate in the grooves. Importantly, these cell-type dependent behaviours were also maintained when in co-culture. We show that it is possible to spatially separate a mixed suspension of two cell types by allowing them to migrate and proliferate on a substrate with engineered microtopographies. This ability may have important implications for investigating the mechanisms that facilitate cellular topographic sensing. Moreover, our results may provide insights towards the controlled development of complex three-dimensional multi-cellular constructs.

© 2013 Elsevier Ltd. All rights reserved.

1. Introduction

The physical properties of the cellular microenvironment play a crucial role in governing numerous critical physiological and pathological pathways [1–5]. In vivo, cells are exposed to and reside in an intricate mesh of proteins known as the extracellular matrix (ECM) [6]. It is well known that complex physical and biochemical interactions between cells and their ECM regulate differentiation, proliferation and migration [1–5]. Moreover, the physical properties of the ECM, such as matrix topography and mechanical properties, also play a major role in modulating cell biology [7–14]. In the laboratory, cells are traditionally cultured on flat two-dimensional surfaces. In comparison to the in vivo matrix microenvironment, these surfaces often lack the complex nano- and micro-scale topographies found in vivo. Indeed, engineered substrates with tunable nano- and micro-scale topographies are now becoming extensively employed in many studies [7–28]. Substrate topography can be modulated in

numerous ways, including altering surface roughness through chemical or plasma treatments to creating long-range ordered features with micro- and nano-scale fabrication approaches [28].

Cellular responses to nanoscale topographies have been extensively studied and may have the potential in aiding elucidation of complex control mechanisms involved in many biological pathways [18]. Fabricated nanoscale grooves, holes and pillars arranged in ordered patterns or in spatial gradients have all been employed to study cellular responses to topography [7,8,13]. Importantly, as these structures are far smaller than typical cell size, an individual cell will be exposed to many features at any given time. It has been observed that cells display an exquisite sensitivity to nanoscale changes in aspect ratio, density and spacing of these features, often in a cell-type dependent manner [7–14]. For example, nanoscale grooves will affect the alignment and migration dynamics of many cell types (such as fibroblasts, neurons and smooth muscle cells) [7,8,13]. This is a process known as contact guidance [29] and has been observed in response to both micro- and nano-scale topographic features. In vivo, migration is extremely important in many physiological and pathological processes (such as cancer metastasis, wound healing and embryogenesis) and is highly sensitive to the nanotopography of the ECM [7,8,13]. In addition to cell

* Corresponding author. Department of Physics, MacDonald Hall, 150 Louis Pasteur, University of Ottawa, Ottawa, ON K1N 6N5, Canada. Tel.: +1 613 562 5800x6965; fax: +1 613 562 5190.

E-mail address: a@pellinglab.net (A.E. Pelling).

morphology and migrations, nanoscale grooves also modulate sub-cellular organization of the cytoarchitecture as well as numerous signalling pathways [19,22,27]. In several cases, cell proliferation has also been observed to display a sensitivity to substrate topography in many cell types [15,30–32]. Finally, during very complex processes, such as stem cell differentiation, it is becoming clear that stem cell fate is influenced by the integration of a multitude of nanotopographical, physical and biochemical cues [4,15,17,22,23].

In contrast to previous work investigating the role of topographical cues smaller than the typical length scale of a cell, a large number of studies have employed substrates with microscale topographies [11,13,16,20,24–26,28]. In many studies, surfaces containing grooves whose geometries (depth, width and ridge width) can vary in a range of less than 10 μm to greater than 100 μm have been employed to demonstrate effects on cell alignment, migration and organization. Importantly, as the groove sizes become larger than a typical cell, this allows for the appearance of several phenomena. Cells not only align with the direction of the grooves, but have also display bridging behaviour. Bridging behaviour occurs when fibroblast preferentially migrate and proliferate along groove ridges to form bridges from one ridge to another or between the bottom of the groove and the top of a ridge [20,24]. Moreover, bridging also occurs when cells form a connection between the bottom of the groove and the top of a ridge [24]. This type of behaviour is very much dependent on the geometric properties of the grooves and in the case of fibroblasts, at least three distinct geometric regimes of behaviour have been characterized [24].

Here, we microfabricated a series of 50 μm deep grooves with increasing widths (25, 50, 100 and 500 μm) and 100 μm wide ridges. In contrast to previous studies, we compared the influence of these substrates on two distinct cell types (NIH3T3 fibroblast and MDCK epithelial cells). NIH3T3 cells are highly motile and lack the strong cell–cell coupling and tight junctions found in MDCK cells. Therefore, we hypothesized that the two cell types may display distinct responses to substrate topography. Cells were cultured on the grooved substrates and were examined after 4, 24, 48 and 72 h of culture. At each time point we quantified the three-dimensional cellular alignment and organization for each cell type on each substrate. Finally, as multiple cell types are found in close contact in vivo, we also grew co-cultures of cells on the substrates. This approach allowed us to examine the influence of contact guidance in a mixture of fibroblast and epithelial cells.

2. Materials and methods

2.1. Substrate fabrication

Master substrates were created with standard soft photolithography techniques on silicon wafers (Universitywafers.com, USA). The wafers were cleaned with a Piranha wet etch solution (3:1 sulphuric acid:hydrogen peroxide), followed by immersion in de-ionized water and subsequent dehydration by baking at 200 $^{\circ}\text{C}$ for 30 min. SU-8 2015 photoresist (Microchem, USA) was then spin coated to a uniform film thickness of 50 μm . A master mould was created by transferring photomask patterns to the photoresist according to the photoresist manufacturer's protocol. The photomask consisted of separate 2.25 cm^2 square regions each containing 1.5 cm long black lines, spaced every 100 μm . The widths of the lines varied in each region and were either 25, 50 or 100 μm . Polydimethylsiloxane (PDMS) substrates with defined topographies were created by pouring a 1:10 solution of curing agent:elastomer (Sylgard 184, Ellsworth Adhesives) over the photoresist master. The PDMS was allowed to crosslink in a convection oven at 80 $^{\circ}\text{C}$ for 3 h. A schematic of the substrate fabrication process is shown in Fig. 1. To functionalize the PDMS substrates, they were air plasma treated at 30 W for 30 s to generate hydroxyl groups. The substrates were then immediately coated with 5 $\mu\text{g}/\text{cm}^2$ rat-tail collagen I (Gibco), incubated at room temperature for 1 h and then rinsed in PBS. Scanning electron microscopy (SEM) of gold-coated PDMS substrates were acquired with a JEOL JSM-7500F FESEM.

2.2. Cell culture

NIH3T3 mouse fibroblast cells and Madin Darby Canine Kidney (MDCK) epithelial cells were cultured in high glucose DMEM containing 10% Fetal Bovine

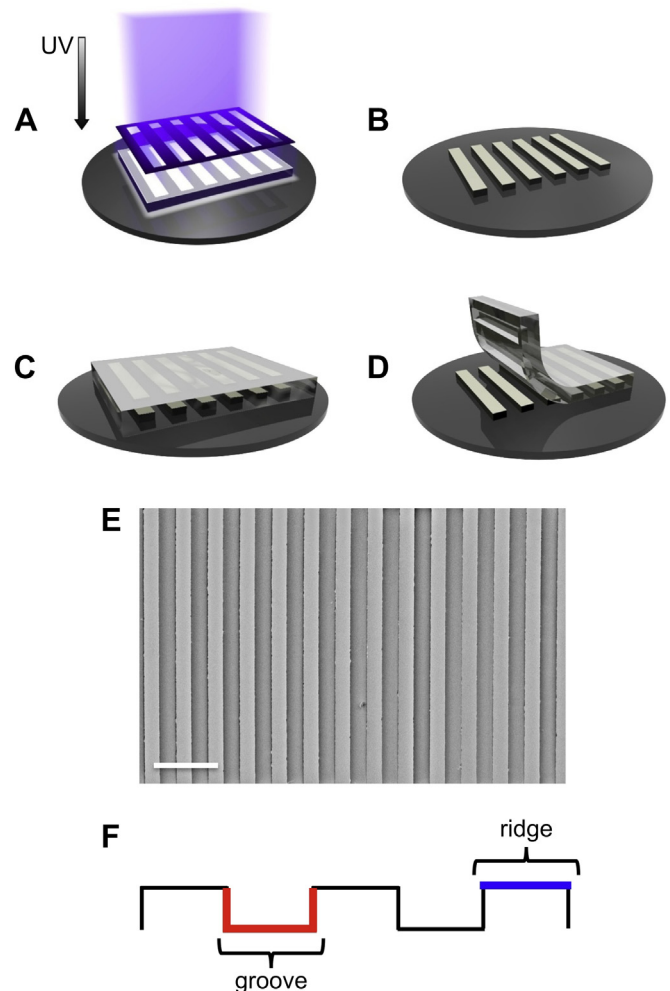


Fig. 1. Microfabrication of microscale grooves in PDMS. (A) After spin coating a 50 μm thick SU8 photoresist onto a silicon wafer, UV light is shone through a mask to crosslink exposed areas. (B) After developing the wafer, un-crosslinked SU8 is removed leaving behind rectangular features. (C) PDMS is poured over the features and cured. (D) The PDMS is then peeled from the substrate and the substrate microtopography is then functionalized with collagen. (E) A top-down SEM image of the PDMS substrate reveals the structure of a typical microtopography with 100 μm grooves and ridges. (F) For the purposes of this study we defined cells as in a 'groove' (red region) or on a 'ridge' (blue region), as shown in the schematic. (For interpretation of the references to colour in this figure legend, the reader is referred to the web version of this article.)

Serum (FBS) and 1% penicillin/streptomycin antibiotics (all from Hyclone). The cells were cultured at 37 $^{\circ}\text{C}$ and 5% CO_2 in 100 mm dishes. For experiments, functionalized PDMS substrates were placed into 35 mm diameter dishes and the cells were seeded at a density of 20,000 cells/ cm^2 . Cells were grown for either 4, 24, 48 or 72 h before inspection. For co-culture experiments, an equal number of NIH3T3 and MDCK cells were thoroughly mixed and then seeded and imaged in the same manner as mono-culture experiments.

2.3. Immunofluorescence staining, live cell staining and microscopy

Cells cultured on PDMS substrates were fixed with 3.5% paraformaldehyde and permeabilized with Triton X-100 at 37 $^{\circ}\text{C}$. Cells were stained for actin using phalloidin conjugated to Alexa Fluor 546 (Invitrogen) and DNA was stained using DAPI (Invitrogen). A full protocol has been published previously [33]. Samples were then mounted using Vectashield (Vector Labs) and a #1 coverslip placed on top of the PDMS substrate. The sample was inverted and then imaged with confocal microscopy. In co-culture NIH3T3 cells were pre-loaded with the live cell dye CellTracker Green CMFDA (Invitrogen) following manufacturer protocols and cultured with MDCK cells for 4 or 48 h. After the allotted time in culture, all cells were loaded with live cell nuclear stain, Hoechst 33342 (Invitrogen). In some cases co-cultures were imaged live with a Nikon Ti-E inverted phase contrast and fluorescence microscope with a long working distance 40 \times objective or they were fixed (but not

permeabilized) and mounted in Vectashield. Fixed samples were imaged on a Nikon Ti-E A1-R high-speed resonant laser scanning confocal microscope (LSCM) with a phase contrast 10× NA0.3 objective or a DIC 60× NA1.2 water immersion objective. Bare PDMS substrates were also imaged with Scanning Electron Microscopy (SEM).

2.4. Image and statistical analysis

All images were analysed with ImageJ. Cell nuclei were manually counted in order to quantify the numbers of cells proliferating in the grooves or on the ridges. The degree of cell alignment with respect to the groove direction was quantified by first thresholding confocal images of cell nuclei. An ellipse was fit to each identified nucleus and the angle between the major axis of the ellipse and the groove direction was determined with the ImageJ Analyze Particles plugin. The second order Legendre polynomial was employed to quantify the average degree of alignment with the groove direction within the cell population. All values in the text are presented as the average \pm s.e.m. A one-way ANOVA followed by a Tukey test for means comparison or two-sample *t*-tests were performed to assess significance ($p < 0.05$).

3. Results

3.1. Microfabricated substrates with microscale topography for cellular confinement

In this study, the effects of micron scale surface topography and confinement on cell localization were investigated with PDMS substrates. Substrates were fabricated using standard soft lithography procedures (Fig. 1A–E). In all cases cells were seeded onto substrates that possessed a surface topography with 50 μm deep grooves and 100 μm wide ridges (Fig. 1F). The ridges were spaced at defined pitch to create 25, 50 or 100 μm grooves. In this context, cells are exposed to confinement geometries that are ~ 2 – 10 times larger than the typical length scale of an individual cell. Cells were then imaged 4, 24, 48 and 72 h after seeding to investigate how microscale confinement affects cellular localization. In contrast to previous studies, here we investigated the response of two cell types (NIH3T3 fibroblast and MDCK epithelial cells) alone or in co-culture. These cell types were specifically chosen, as NIH3T3 fibroblasts are highly motile [34,35], whereas MDCK epithelial cells are strongly interacting, forming strong cell–cell contacts and stable monolayers [36,37]. For the purposes of this study, we defined localization in the grooves if cells were found on the bottom or sidewall surfaces occurring between the ridges (Fig. 1E). Conversely, localization on ridges was defined as cells being found on the top 100 μm ridge surface (Fig. 1E). In both cases, minutes after seeding, cells were always found to sink to the bottom of the grooves, simply due to their higher density than the surrounding medium. In this initial state, cells were easily confined to the grooves by the 50 μm ridge height. Cells were then placed in a culture incubator and examined at the time points described above. The 4-h time point was found to be the earliest time at which cell–surface interactions were strong enough to allow for reproducible staining and imaging.

3.2. Cell type dependent responses to microscale confinement

At each time point, cellular actin and nuclei were fluorescently labelled and imaged with laser scanning confocal microscopy (LSCM). LSCM images provide information on the three-dimensional location of individual cells in the microscale features. In this study, we quantified the number of cells found on the ridges or within the grooves. A total of $n = 3$ independent substrates were prepared for each groove width and 3 randomly chosen regions were imaged on each sample with LSCM. Therefore, we counted cell locations in a total of 9 images for each groove width and each cell type. NIH3T3 cells display a clear response to surface topography for all groove widths (Fig. 2A–C). In all cases, we have false-coloured the actin of cells found within the grooves (red) and on the ridges (green) in order to provide a visual reference. NIH3T3

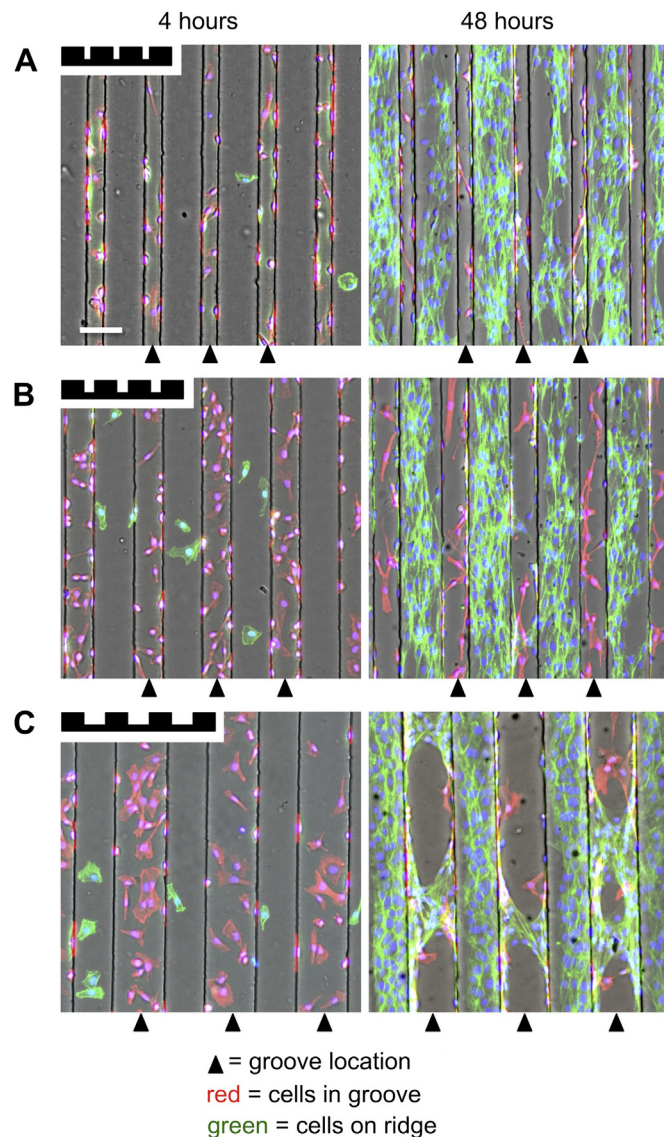


Fig. 2. NIH3T3 cells were cultured on the (A) 25 μm , (B) 50 μm and (C) 100 μm wide grooves for 4, 24, 48 and 72 h, subsequently stained for actin and cell nuclei and imaged the LSCM. Nuclei are shown in blue and actin is coloured red for cells growing within the grooves and coloured green for cells growing on the ridges (triangles indicate the grooves). Images are shown for cells cultured for 4 and 48 h. Triangles indicate the bottom surface of the grooves. Scale bar in (A) = 100 μm and applies to all. NIH3T3 cells display a clear preference for migrating and proliferating on the ridges. (For interpretation of the references to colour in this figure legend, the reader is referred to the web version of this article.)

cells are found to be highly localized within the grooves after 4 h of culture time, however, by 48 h, cells have migrated specifically to the ridges and become highly confluent. It is clear that after 48 h of culture, NIH3T3 cells display a clear preference to the ridge surfaces. Very few cells are found within the grooves even though the ridges are highly crowded. In some cases cells were observed to form ridge-to-ridge ridges over grooves, consistent with previous studies [20,24]. On the other hand, a vastly different response is observed in MDCK cells (Fig. 3A–C). Consistent with the NIH3T3 cells, MDCK cells are found in large numbers in the grooves after only 4 h of culture. However, after 48 h of culture, MDCK cells continue to be found in the grooves in high proportions and at high density, whereas only a small fraction of cells are found on the

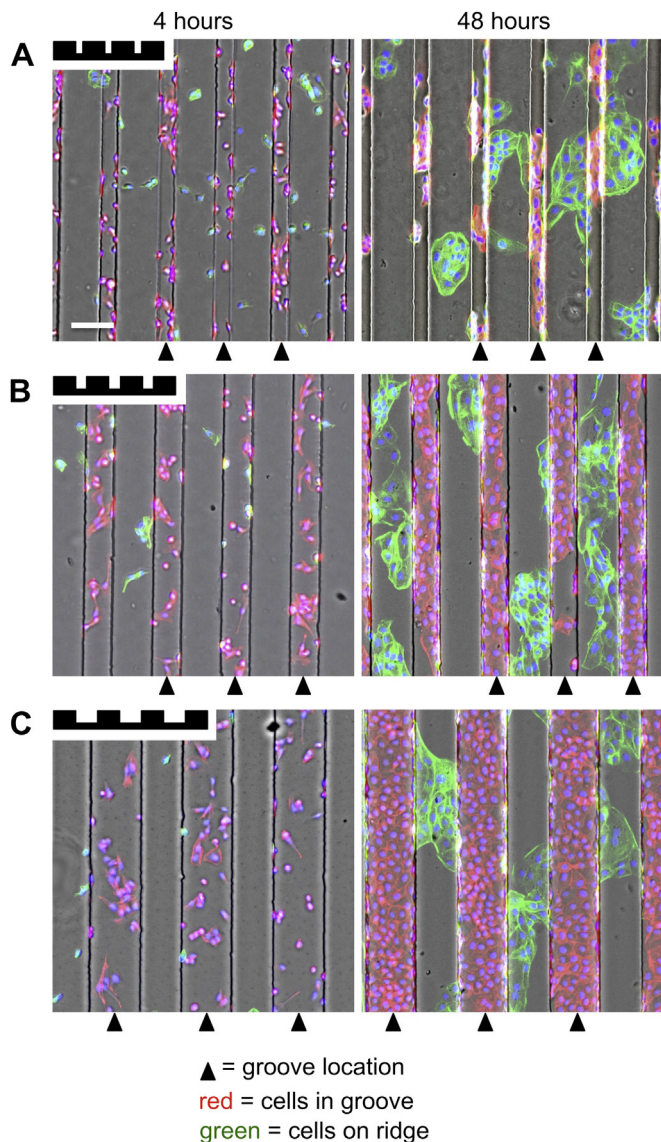


Fig. 3. MDCK cells were cultured on the (A) 25 μm , (B) 50 μm and (C) 100 μm wide grooves for 4, 24, 48 and 72 h, subsequently stained for actin and cell nuclei and imaged the LSCM. Nuclei are shown in blue and actin is coloured red for cells growing within the grooves and coloured green for cells growing on the ridges (triangles indicate the grooves). Images are shown for cells cultured for 4 and 48 h. Triangles indicate the bottom surface of the grooves. Scale bar in (A) = 100 μm and applies to all. MDCK cells display a clear preference for migrating and proliferating within the grooves. (For interpretation of the references to colour in this figure legend, the reader is referred to the web version of this article.)

ridges by 48 h. Clearly, these two cell types display distinct responses to confinement in microscale geometries.

Using the nuclei to count cells, we calculated the ratio of the number of cells growing on the ridges to the number of cells growing in the grooves, as a function of time, for all substrate geometries. The Ridge/Groove ratio reveals that after ~ 24 h of culture, the majority of NIH3T3 cells are found preferentially on the ridges (Ridge/Groove ratio > 1) on substrates with 25 μm and 50 μm wide grooves in comparison to the 100 μm grooves (Fig. 4A). After 48 h of culture a statistically significant difference appears when comparing the Ridge/Groove ratio between the 100 μm and the 25 μm grooves ($p < 0.01$) but not the 50 μm grooves ($p > 0.9$). However, by the 72 h time point, the Ridge/Groove ratio approaches

~ 2 in all cases with no significant dependence on groove width ($p > 0.2$ in all cases). In contrast, MDCK cells display a different response to microscale topography when compared to NIH3T3 cells. In all cases, the Ridge/Groove ratio slowly approaches 1 over the 72 h time course (Fig. 4B). However, cells cultured on the 25 μm grooves approach 1 more rapidly and become significantly different from the 50 μm and 100 μm grooves by 48 h of growth ($p < 0.05$ in both cases). Similar to the NIH3T3 cells, there is no statistically significant dependence of the Ridge/Groove ratio on groove width ($p > 0.2$ in all cases). Importantly, when NIH3T3 cells are cultured on substrates where the groove width is increased to 500 μm , cells no longer display any preference for migrating and proliferating on the ridges (Fig. 4C). Unsurprisingly, MDCK cells are still found within the 500 μm grooves (Fig. 4D).

Finally, when cells were allowed to propagate until covering the entire surface (~ 120 h of growth), two distinct morphologies were observed. NIH3T3 (Fig. 5A, B) and MDCK (Fig. 5C, D) cells growing to confluence on the 50 μm grooves and are representative of the morphologies observed on the 25 and 100 μm grooves. In the case of MDCK cells, a complete cell monolayer formed after 120 h and covered the entire grooved substrate. The monolayer was observed to match the surface topography with cells observed along all surfaces of the grooves and ridges. Conversely, NIH3T3 cells were first observed to grow to confluence along the ridges, eventually forming bridges. After 120 h of culture cells were observed to completely fill the grooves.

3.3. Cellular alignment in microscale grooves

In order to quantify cellular alignment we characterized the orientation of cell nuclei computationally by first calculating the angle (θ) formed between the long axis of each elliptical nucleus and the groove direction. We then calculated the degree of alignment by using an approach commonly employed when characterizing the preferred directionality in liquid crystals. The average value of the second order Legendre polynomial was calculated using the orientation of each nucleus in a field of view [38]:

$$s = \left\langle \frac{3\cos^2\theta - 1}{2} \right\rangle$$

In a given population of cells, S will approach 0 if they are randomly oriented with respect to the groove direction. Conversely, S will approach 1 if there is a strong degree of alignment between the groove direction and the cells. Finally, if the cells are aligned perpendicular to the groove direction, S will approach -0.5 . Therefore, S provides a quantitative measure of the degree of alignment parallel or perpendicular to the groove direction or if the cell population lacks significant alignment. NIH3T3 or MDCK cells were allowed to proliferate on 25, 50, 100 and 500 μm wide grooves for 48 h at which point the cells were fixed and stained. A total of $n = 3$ independent substrates were prepared for each groove width and 3 randomly chosen regions were imaged on each sample with LSCM. Therefore, an average order parameter was calculated from cells in a total of 9 images for each groove width and each cell type (Fig. 6). NIH3T3 cells displayed a strong degree of alignment ($S = 0.80 \pm 0.04$), with no significant dependence on the 25, 50 and 100 μm grooves ($p > 0.6$ in all cases). On the other hand, MDCK cells displayed a smaller degree of alignment ($S = 0.58 \pm 0.04$) compared to NIH3T3 cells ($p < 0.01$ in all cases), with no significant dependence on groove widths ($p > 0.3$ in all cases). Finally, NIH3T3 and MDCK cells cultured on grooves of 500 μm displayed a statistically significant decrease in alignment compared to the 25, 50 and 100 μm grooves ($S = 0.30 \pm 0.03$ and 0.36 ± 0.03 , respectively, $p < 0.01$ in all cases) with no cell-type dependence ($p > 0.7$).

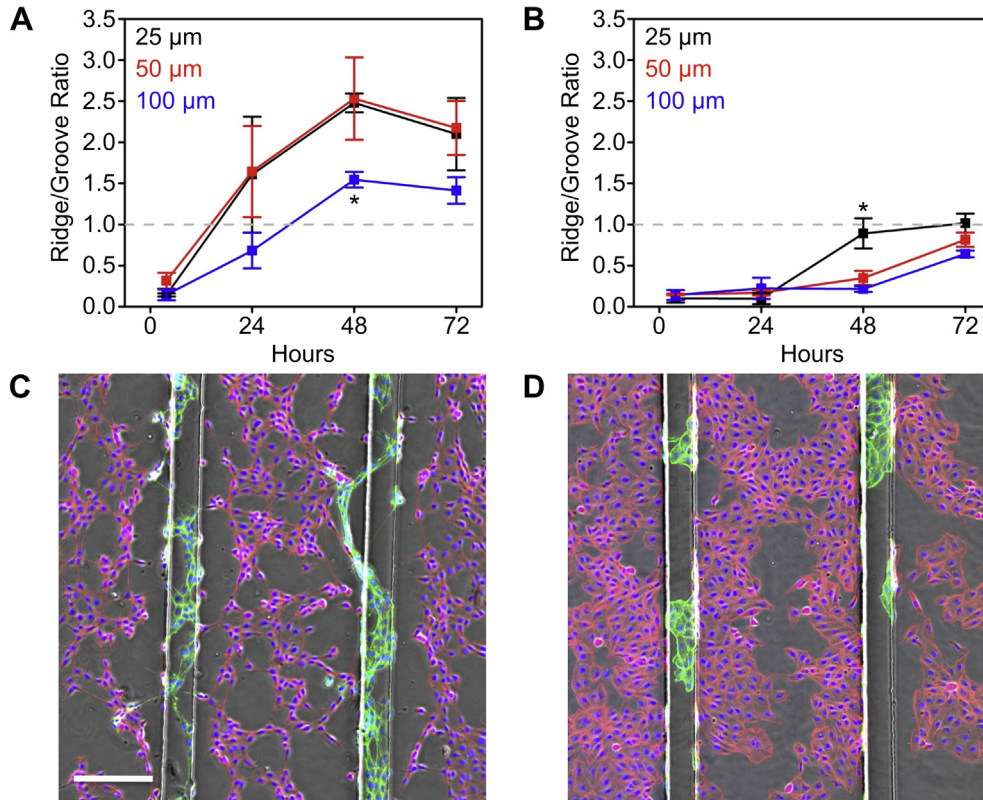


Fig. 4. The number of cell growing within the grooves or on the ridges was determined and a Ridge/Groove ratio was calculated for the 25 μm (black), 50 μm (red) and 100 μm (blue) wide grooves. (A) The Ridge/Groove ratio for NIH3T3 cells demonstrates that the cells rapidly move to the ridges. By 48 h the Ridge/Groove ratio is significantly (*) higher for the 25 and 50 μm grooves compared to the 100 μm grooves. (B) The Ridge/Groove ratio for MDCK cells demonstrates that the cells preferentially localize within the grooves. By 48 h, the Ridge/Groove ratio is significantly (*) higher for the 25 μm grooves compared to the 50 and 100 μm grooves. (C) NIH3T3 and (D) MDCK cells cultured on 500 μm wide grooves for 48 h (scale bar = 250 μm and applies to both images). Nuclei are shown in blue and actin is coloured red for cells within the grooves and green for cells are on the ridges. (For interpretation of the references to colour in this figure legend, the reader is referred to the web version of this article.)

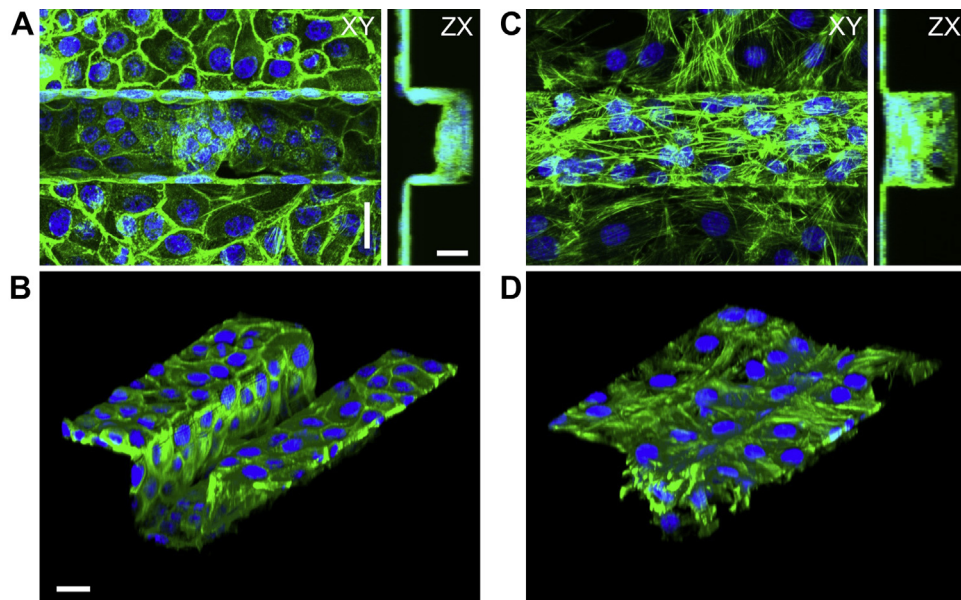


Fig. 5. Images of actin (green) and nuclei (blue) for (A, B) MDCK and (C, D) NIH3T3 cells after growing for 120 h on 50 μm wide grooves (scale bars = 25 μm and apply to all, results are representative of all groove sizes). MDCK cells form a continuous two-dimensional sheet, closely matching substrate topography whereas NIH3T3 cells fill the grooves and completely cover the substrate. This behaviour is clearly observed in the three-dimensional rendering of the LSCM data in (B) and (D). (For interpretation of the references to colour in this figure legend, the reader is referred to the web version of this article.)

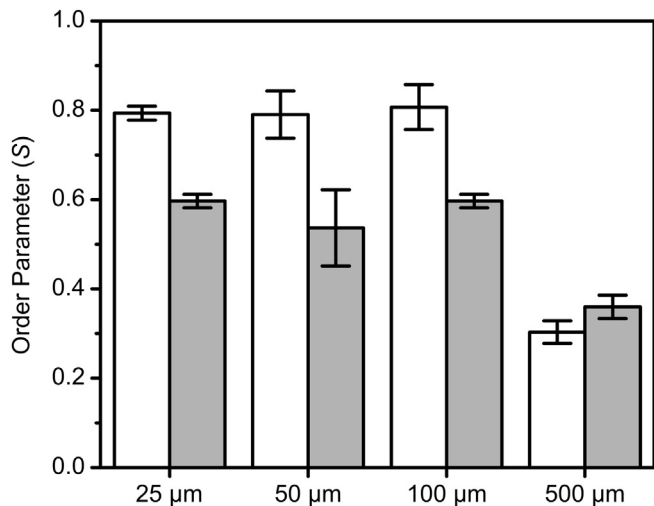


Fig. 6. An order parameter (S) was calculated for NIH3T3 (white bars) and MDCK (grey bars) using cell nuclei as indicators of orientation with respect to the groove direction. An order parameter approaching 1 indicates a high degree of parallel alignment between cells and the groove direction. Conversely, an order parameter approaching 0 indicates a high degree of perpendicular alignment between cells and the groove direction. On the 25, 50 and 100 μm grooves, both cell types display a strong degree of alignment with the groove direction. Conversely, alignment was significantly diminished on the 500 μm grooves.

3.4. Confinement guidance in co-cultures

To further investigate the cellular response to confinement, we co-cultured NIH3T3 and MDCK cells and exposed them to substrates with defined microscale topography. In all cases, NIH3T3 cells were pre-loaded with a green fluorescent cell tracker dye prior to co-culture and prior to imaging, all cell nuclei were labelled with the DNA specific Hoechst 33342. This approach allowed us to positively identify individual cells as either NIH3T3 or MDCK. Imaging reveals that even in the presence of a co-culture, the majority of cells continued to display a clear preference for growing on the ridges or in the grooves. Phase contrast and fluorescence imaging reveals that after 48 h of co-culture on 100 μm wide grooves, NIH3T3 cells display a clear preference to migrate and grow on the ridge surfaces (Fig. 7A). At the same time, MDCK cells are clearly observed in the grooves (Fig. 7B). This is in contrast to co-cultured cells grown on flat PDMS surfaces. In this case NIH3T3 and MDCK cells are observed to distribute heterogeneously (Fig. 7C).

4. Discussion

Physical cues in the cellular microenvironment such as substrate topography and mechanical properties have a significant role in regulating physiological and pathological processes [1–5]. In addition, it has also been shown that flat substrates patterned with ECM proteins can be used to control cell shape, alignment, proliferation and differentiation [14,25,30,39]. Recently, cells exposed to either microscale grooves or microscale lines of fibronectin were observed to align along the presented patterns [25]. However, when a substrate of grooves fabricated in one direction was overlaid with lines of fibronectin in the orthogonal direction, cells were observed to preferentially align with the grooves. Therefore, surface topography is an extremely strong cue in regulating living cells, even overcoming the influence of surface patterns of ECM proteins [25] and might even be used as a means of characterizing cellular signalling pathways [18]. Indeed, it has been demonstrated that libraries of substrate topographies can be employed to reveal previously unknown cellular responses to substrate topography [33].

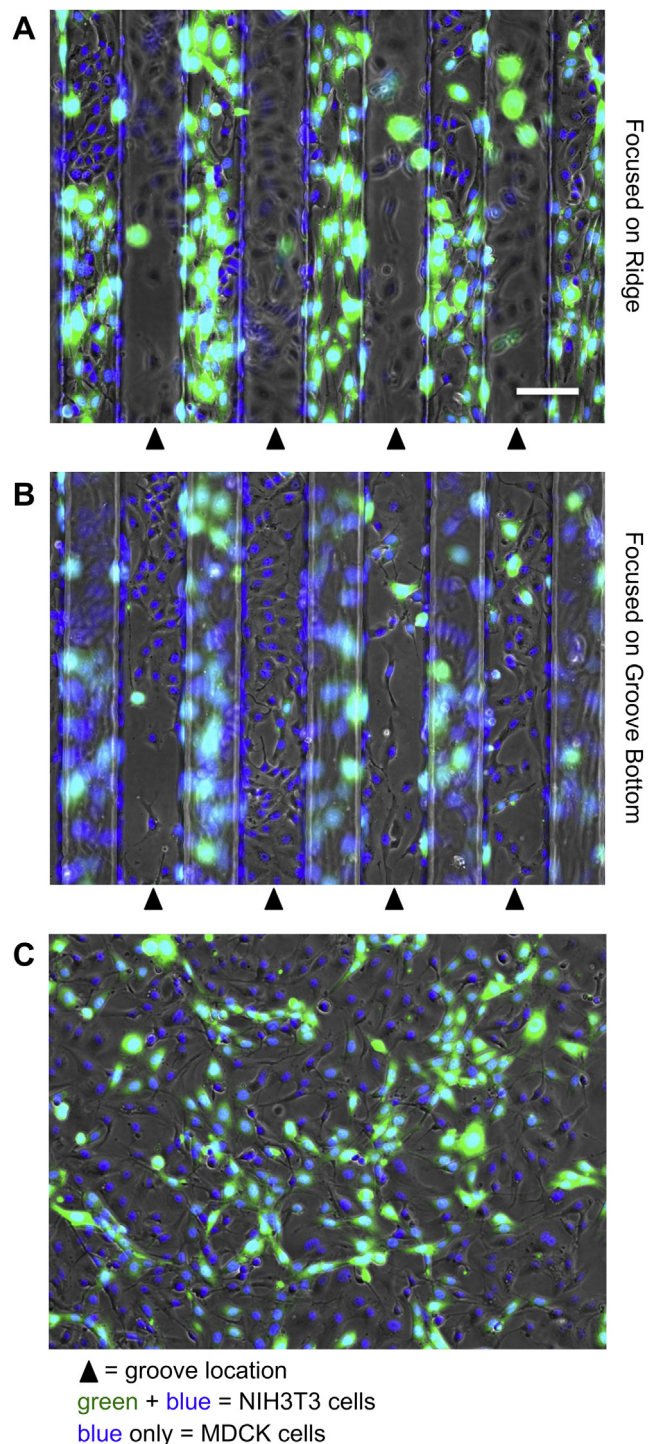


Fig. 7. NIH3T3 cells (green with blue nuclei) and MDCK cells (blue nuclei only) were placed in co-culture and imaged after 48 h (triangles indicate the grooves). Data shown were recorded on 100 μm grooves but is representative for all groove widths. Phase contrast images were recorded when the microscope was focussed on the (A) ridges and (B) bottom surfaces of the grooves and reveals a spatial separation of both cell types (scale bar = 100 μm and applies to all). When co-cultured cells are grown on a flat PDMS surface cells are heterogeneously distributed and no alignment or separation is visible. (For interpretation of the references to colour in this figure legend, the reader is referred to the web version of this article.)

In this study, we examined the influence of microscale topography on the three-dimensional spatial organization and alignment of NIH3T3 fibroblasts and MDCK epithelial cells. PDMS substrates were fabricated with grooves of varying widths (25, 50 and 100 μm)

and constant depth (50 μm) and ridge width (100 μm). NIH3T3 fibroblasts displayed a clear preference for proliferating on the ridges, consistent with previous studies [20,24]. On the other hand, MDCK epithelial cells preferentially proliferated inside the grooves, a result that has not been observed previously to our knowledge. However, nanoscale grooves are well known to exhibit contact guidance on cultured epithelial cells [7,8,13]. In all cases, our substrates were functionalized with collagen and it is well known that aligned collagen fibres, both *in vivo* and *in vitro*, can lead to preferential cellular alignment, migration and contact guidance [7,8,13]. Here, we can rule out collagen-induced contact guidance, as the collagen is likely randomly bound to our substrates after using standard functionalization protocols. In addition, in both cases cellular alignment was lost on the substrates with 500 μm grooves. Alignment was quantified by calculating an order parameter which was shown to vary from ~ 0.8 to ~ 0.6 (fibroblasts and epithelial cells respectively) on the 25, 50 and 100 μm grooves to ~ 0.3 on the 500 μm grooves. Co-cultured cells on flat collagen-functionalized PDMS substrates did not display any preferential alignment. Therefore, it can be reasonably assumed that microtopography, rather than collagen functionalization, produces the observed contact guidance in our study.

We also quantified the preferential three-dimensional spatial localization of cells by simply counting how many were found on the ridge or anywhere within the groove, at each time point, on all substrates. The surface area available to the cells is significantly different on the ridges versus in the grooves. The ridges have a surface area of $1.5\text{ cm} \times 100\text{ }\mu\text{m} = 0.015\text{ cm}^2$ whereas each groove in this study has a surface area of ~ 0.019 , ~ 0.023 and 0.030 cm^2 . If the higher available surface area in the grooves played a major role in cell organization, the observed Ridge/Groove ratio would consistently be less than 1 in all cases. This was clearly not the case when examining NIH3T3 cells. However, this was the case in MDCK cells at all time points and for all groove widths. The Ridge/Groove ratio is initially ~ 0.2 in the first 24 h before rapidly approaching 1 whereas the Ridge/Groove surface area ratio varies from 0.5 to 0.8. Therefore, within the first 24 h of culture, MDCK cells display preferential proliferation within the grooves that cannot be simply explained by an increase in surface area. However, once MDCK cells have proliferated to the point where they can no longer remain confined in the groove, they migrate out and begin proliferating on the ridge surface. At this point the Ridge/Groove ratio approaches 1 and this may simply be a result of the surface area occupied by the cells on each surface. Indeed, MDCK cells were observed to form complete two-dimensional sheets of cells that closely followed substrate topography with no tendency to form multicellular aggregates within the grooves during the timescale of our experiment. In contrast, when allowed to proliferate to confluence over 5 days, NIH3T3 cells were first observed to preferentially grow on the ridges and at later times (>3 days) would form large aggregates within the grooves.

In order to examine the influence of topography on the spatial localization of the cells, we co-cultured both cell types on the grooved substrates. In this case, fibroblasts were pre-loaded with a live cell cytoplasmic green fluorescent dye prior to co-culture. Prior to imaging, all cells were loaded with a blue fluorescent live cell dye specific to DNA. Therefore, during imaging, fluorescent green cells with blue fluorescent nuclei could be positively identified as fibroblasts. On the other hand, cells with blue-fluorescent nuclei alone could be positively identified as epithelial cells. In this case, it was clear after 48 h of proliferation, that cells still displayed a preferential localization on the ridges or in the grooves. However, we note that the separation is not 100% complete. However, despite numerous cell–cell interactions and possible effects associated with the release of cellular factors and signalling molecules,

substrate topography still had a major influence on migration and organization. NIH3T3 cells maintained a preferential alignment and organization on the ridges while MDCK cells were still preferentially found in the grooves. Importantly, when cells were co-cultured on a flat PDMS surface they were organized in a heterogeneous manner after 48 h of proliferation.

There is currently significant interest in using the characteristic of nano- and micro-textured surfaces to control, direct and modulate cell behaviours. Although many studies have revealed that cells are clearly sensitive to substrate topography, the exact underlying molecular mechanism responsible for their ability to sense and respond to topographic cues is still not well understood. It is now clear the regulation of acto-myosin contractility, and perhaps cellular traction forces, form part of the sensing mechanism [22,26,27]. In addition, topography also has a significant impact on the organization, dynamics and regulation of structures involved in coupling the cell to its microenvironment, such as integrins, focal adhesions and the cytoskeleton [22,26,27]. It was recently postulated that one of the forces driving fibroblasts to localize on the ridge of microgrooves is the local oxygen gradient [20]. However, the results on epithelial cells appear to contradict this possibility, assuming their oxygen requirements are similar to fibroblasts. Moreover, in our experiments, several millimetres of liquid exist above the substrate surface and it is unlikely that any change in oxygen concentration in the 50 μm distance between the bottom of the grooves and the ridge will be significant enough to drive the migration of the cells.

We hypothesize that one of the main driving forces that results in the differential response of fibroblasts and epithelial cells is likely cell function. Fibroblasts are highly motile cells and in comparison to epithelial cells, tend to lack the same degree of strong cell–cell coupling and the presence of tight junctions [37,40]. Therefore, we postulate that there would be less physical confinement on the ridges and therefore promote migration. Conversely, in a more physically confined environment, cell–cell contacts are more likely to form thereby inhibiting migration away from the growing cell sheet and promoting proliferation within the groove. Although this explanation does not provide any mechanistic insight, it is supported by the Ridge/Groove ratio data. In the case of fibroblasts, the Ridge/Groove ratio on 100 μm wide grooves does not increase as rapidly as the 25 and 50 μm grooves. In this case, the 100 μm grooves are just as wide as the ridges, however the degree of confinement within the 50 μm deep well appears to drive migration out of the groove and onto the ridge. Conversely, epithelial cells are forced onto the ridge as they quickly fill the 25 μm grooves in comparison to the 50 and 100 μm grooves. The wider 50 and 100 μm grooves allow for prolonged cell proliferation within the grooves before being forced out onto the ridges. Therefore, although substrate topography can act as a stronger environmental cue than substrate biochemistry [25], clearly cell function and physiology play an equally important role in dictating the response to topographic information in the microenvironment.

5. Conclusion

This study has revealed that topographic cues can lead to the three dimensional spatial separation of two cell types. Fibroblasts displayed a clear preference for migrating and proliferating on the ridges of microscale grooves whereas epithelial cells preferentially migrated and proliferated in the microscale grooves. Importantly, the cell-type dependent behaviour observed here is also maintained when fibroblasts and epithelial cells were co-cultured. Physical confinement also appears to be playing an important role in driving cell-type dependent responses to micro-topographies. This is consistent with previous work demonstrating

that confinement and encapsulation of cells in engineered three-dimensional hydrogels can drive their organization and fate. The ability to pattern and organize at least two distinct cell types in three-dimensions may have important implications for investigating the mechanisms of cellular organization and proliferation. Moreover, the phenomena described here may find utility in the development of biomaterials that can direct the complex three-dimensional growth and behaviour of cells in complex artificial tissue constructs.

Acknowledgements

A.L. acknowledges support from the Natural Sciences and Engineering Research Council (NSERC) Undergraduate Student Research Award and the University of Ottawa Undergraduate Research Opportunities Program. D.T. thanks the Fond de recherche du Québec: Nature et Technologie (FQRNT) and Mitacs Elevate Program. A.E.P. acknowledges generous support from a Province of Ontario Early Researcher Award and a Canada Research Chair (CRC). This work was made possible by funding from the Canadian Foundation for Innovation (M.G. and A.E.P.), NSERC Discovery Grants (M.G. and A.E.P.), an NSERC Discovery Accelerator Supplement (A.E.P.) and a CRC Operating Grant (A.E.P.). The authors wish to thank Dr. Yun Liu for assistance with SEM imaging.

References

- Janmey PA, Miller RT. Mechanisms of mechanical signaling in development and disease. *J Cell Sci* 2011;124:9–18.
- Bukoreshtliev NV, Haase K, Pelling AE. Mechanical cues in cellular signalling and communication. *Cell Tissue Res* 2013;352:77–94.
- Buxboim A, Ivanovska IL, Discher DE. Matrix elasticity, cytoskeletal forces and physics of the nucleus: how deeply do cells 'feel' outside and in? *J Cell Sci* 2010;123:297–308.
- Discher DE, Mooney DJ, Zandstra PW. Growth factors, matrices, and forces combine and control stem cells. *Science* 2009;324:1673–7.
- Holle AW, Engler AJ. More than a feeling: discovering, understanding, and influencing mechanosensing pathways. *Curr Opin Biotechnol* 2011;22: 648–54.
- Hynes RO. The extracellular matrix: not just pretty fibrils. *Science* 2009;326: 1216–9.
- Kim DH, Provenzano PP, Smith CL, Levchenko A. Matrix nanotopography as a regulator of cell function. *J Cell Biol* 2012;197:351–60.
- Bettinger CJ, Langer R, Borenstein JT. Engineering substrate topography at the micro- and nanoscale to control cell function. *Angew Chem Int Ed Engl* 2009;48:5406–15.
- Curtis A, Wilkinson C. Topographical control of cells. *Biomaterials* 1997;18: 1573–83.
- Clark P, Connolly P, Curtis AS, Dow JA, Wilkinson CD. Cell guidance by ultrafine topography in vitro. *J Cell Sci* 1991;99:73–7.
- Clark P, Connolly P, Curtis AS, Dow JA, Wilkinson CD. Topographical control of cell behaviour: II. Multiple grooved substrata. *Development* 1990;108: 635–44.
- Clark P, Connolly P, Curtis AS, Dow JA, Wilkinson CD. Topographical control of cell behaviour. I. Simple step cues. *Development* 1987;99:439–48.
- Kulangara K, Leong KW. Substrate topography shapes cell function. *Soft Matter* 2009;5:4072–6.
- Wong JY, Leach JB, Brown XQ. Balance of chemistry, topography, and mechanics at the cell-biomaterial interface: issues and challenges for assessing the role of substrate mechanics on cell response. *Surf Sci* 2004;570:119–33.
- Chen W, Villa-Diaz LG, Sun Y, Weng S, Kim JK, Lam RH, et al. Nanotopography influences adhesion, spreading, and self-renewal of human embryonic stem cells. *ACS Nano* 2012;6:4094–103.
- Greco F, Fujie T, Ricotti L, Taccola S, Mazzolai B, Mattoli V. Microwrinkled conducting polymer interface for anisotropic multicellular alignment. *ACS Appl Mater Interfaces* 2013;5:573–84.
- Teo BK, Wong ST, Lim CK, Kung TY, Yap CH, Ramagopal Y, et al. Nanotopography modulates mechanotransduction of stem cells and induces differentiation through focal adhesion kinase. *ACS Nano* 2013;7:4785–98.
- Unadkat HV, Hulsman M, Cornelissen K, Papenburg BJ, Truckenmuller RK, Carpenter AE, et al. An algorithm-based topographical biomaterials library to instruct cell fate. *Proc Natl Acad Sci U S A* 2011;108:16565–70.
- Seo CH, Furukawa K, Montagne K, Jeong H, Ushida T. The effect of substrate microtopography on focal adhesion maturation and actin organization via the rhoA/ROCK pathway. *Biomaterials* 2011;32:9568–75.
- Su WT, Liao YF, Chu IM. Observation of fibroblast motility on a micro-grooved hydrophobic elastomer substrate with different geometric characteristics. *Micron* 2007;38:278–85.
- Biggs MJ, Richards RG, Dalby MJ. Nanotopographical modification: a regulator of cellular function through focal adhesions. *Nanomedicine* 2010;6:619–33.
- Gerecht S, Bettinger CJ, Zhang Z, Borenstein JT, Vunjak-Novakovic G, Langer R. The effect of actin disrupting agents on contact guidance of human embryonic stem cells. *Biomaterials* 2007;28:4068–77.
- Kulangara K, Yang Y, Yang J, Leong KW. Nanotopography as modulator of human mesenchymal stem cell function. *Biomaterials* 2012;33:4998–5003.
- Stevenson PM, Donald AM. Identification of three regimes of behavior for cell attachment on topographically patterned substrates. *Langmuir* 2009;25: 367–76.
- Charest JL, Eliason MT, Garcia AJ, King WP. Combined microscale mechanical topography and chemical patterns on polymer cell culture substrates. *Biomaterials* 2006;27:2487–94.
- Uttayarat P, Toworfe GK, Dietrich F, Lelkes PI, Composto RJ. Topographic guidance of endothelial cells on silicone surfaces with micro- to nanogrooves: orientation of actin filaments and focal adhesions. *J Biomed Mater Res A* 2005;75:668–80.
- Frey MT, Tsai IY, Russell TP, Hanks SK, Wang YL. Cellular responses to substrate topography: role of myosin II and focal adhesion kinase. *Biophys J* 2006;90:3774–82.
- Lim JY, Donahue HJ. Cell sensing and response to micro- and nanostructured surfaces produced by chemical and topographic patterning. *Tissue Eng* 2007;13:1879–91.
- Weiss P. Cell contact. In: Bourne GH, Danielli JF, editors. *International review of cytology*. Academic Press; 1958. p. 391–423.
- Chen CS, Mrksich M, Huang S, Whitesides GM, Ingber DE. Geometric control of cell life and death. *Science* 1997;276:1425–8.
- Lim JY, Hansen JC, Siedlecki CA, Runt J, Donahue HJ. Human foetal osteoblastic cell response to polymer-demixed nanotopographic interfaces. *J R Soc Interface* 2005;2:97–108.
- Milner KR, Siedlecki CA. Fibroblast response is enhanced by poly(L-lactic acid) nanotopography edge density and proximity. *Int J Nanomedicine* 2007;2: 201–11.
- Guolla L, Bertrand M, Haase K, Pelling AE. Force transduction and strain dynamics in actin stress fibres in response to nanonewton forces. *J Cell Sci* 2012;125:603–13.
- Doyle AD, Kutys ML, Conti MA, Matsumoto K, Adelstein RS, Yamada KM. Micro-environmental control of cell migration—myosin IIA is required for efficient migration in fibrillar environments through control of cell adhesion dynamics. *J Cell Sci* 2012;125:2244–56.
- Kumar G, Meng JJ, Ip W, Co CC, Ho CC. Cell motility assays on tissue culture dishes via non-invasive confinement and release of cells. *Langmuir* 2005;21: 9267–73.
- Gaush CR, Hard WL, Smith TF. Characterization of an established line of canine kidney cells (MDCK). *Proc Soc Exp Biol Med* 1966;122:931–5.
- Gonzalez-Mariscal L, Chavez de Ramirez B, Cerejido M. Tight junction formation in cultured epithelial cells (MDCK). *J Membr Biol* 1985;86:113–25.
- Aratyn-Schaus Y, Oakes PW, Gardel ML. Dynamic and structural signatures of lamellar actomyosin force generation. *Mol Biol Cell* 2011;22:1330–9.
- Zatti S, Zoso A, Serena E, Luni C, Cimetta E, Elvassore N. Micropatterning topology on soft substrates affects myoblast proliferation and differentiation. *Langmuir* 2012;28:2718–26.
- Izumi Y, Hirose T, Tamai Y, Hirai S, Nagashima Y, Fujimoto T, et al. An atypical PKC directly associates and colocalizes at the epithelial tight junction with ASIP, a mammalian homologue of *Caenorhabditis elegans* polarity protein PAR-3. *J Cell Biol* 1998;143:95–106.